ACCOUNTS of chemical research

Article

pubs.acs.org/accounts

Understanding Boron through Size-Selected Clusters: Structure, Chemical Bonding, and Fluxionality

Alina P. Sergeeva,[†] Ivan A. Popov,[†] Zachary A. Piazza,[‡] Wei-Li Li,[‡] Constantin Romanescu,[‡] Lai-Sheng Wang,*[,‡] and Alexander I. Boldyrev*[,†]

[†]Department of Chemistry and Biochemistry, Utah State University, Logan, Utah 84322, United States

[‡]Department of Chemistry, Brown University, Providence, Rhode Island 02912, United States

CONSPECTUS: Boron is an interesting element with unusual polymorphism. While three-dimensional (3D) structural motifs are prevalent in bulk boron, atomic boron clusters are found to have planar or quasi-planar structures, stabilized by localized two-center−two-electron (2c−2e) σ bonds on the periphery and delocalized multicenter−two-electron (nc−2e) bonds in both σ and π frameworks. Electron delocalization is a result of boron's electron deficiency and leads to fluxional behavior, which has been observed in B_{13}^+ and B_{19}^-. A unique capability of the in-plane rotation of the inner atoms against the periphery of the cluster in a chosen direction by employing circularly polarized infrared radiation has been suggested. Such fluxional behaviors in boron clusters are interesting and have been proposed as molecular Wankel motors. The concepts of aromaticity and antiaromaticity have been extended beyond organic chemistry to planar boron clusters. The validity of these concepts in understanding the electronic structures of boron clusters is evident in the striking similarities of the π-systems of planar boron clusters to those of polycyclic aromatic hydrocarbons, such as benzene, naphthalene, coronene, anthracene, or phenanthrene. Chemical bonding models developed for boron clusters not only allowed the rationalization of the stability of boron clusters but also lead to the design of novel metal-centered boron wheels with a record-setting planar coordination number of 10. The unprecedented highly coordinated borometallic molecular wheels provide insights into the interactions between transition metals and boron and expand the frontier of boron chemistry. Another interesting feature discovered through cluster studies is boron transmutation. Even though it is well-known that B^-, formed by adding one electron to boron, is isoelectronic to carbon, cluster studies have considerably expanded the possibilities of new structures and new materials using the B^-/C analogy. It is believed that the electronic transmutation concept will be effective and valuable in aiding the design of new boride materials with predictable properties.

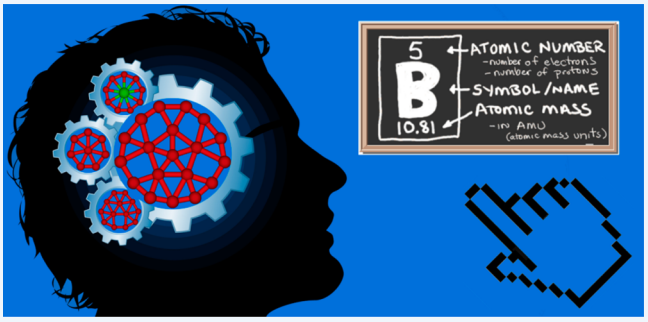

The study of boron clusters with intermediate properties between those of individual atoms and bulk solids has given rise to a unique opportunity to broaden the frontier of boron chemistry. Understanding boron clusters has spurred experimentalists and theoreticians to find new boron-based nanomaterials, such as boron fullerenes, nanotubes, two-dimensional boron, and new compounds containing boron clusters as building blocks. Here, a brief and timely overview is presented addressing the recent progress made on boron clusters and the approaches used in the authors' laboratories to determine the structure, stability, and chemical bonding of size-selected boron clusters by joint photoelectron spectroscopy and theoretical studies. Specifically, key findings on all-boron hydrocarbon analogues, metal-centered boron wheels, and electronic transmutation in boron clusters are summarized.

1. INTRODUCTION

Bulk boron and boron compounds have a vast range of applications from superhard materials and semiconductors to biological compounds with antiseptic, antiviral, antitumor, and antifungal properties. Boron flourishes with a number of polymorphs[1] consisting of B_{12}-icosahedral building blocks, though only four pure elemental phases have been synthesized.[2] Pure boron clusters exhibit planar or quasi-planar structures.[3−28] Influenced by the well documented incidence of carbon based nanostructures in the literature, theoreticians began investigating similar concepts in boron chemistry as evidenced by work on the proposed boron buckyball, volleyball, and other fullerenes,[29−34] two-dimensional sheets,[35−43] nanotubes,[44] nanoribbons,[45] and core−shell stuffed boron fullerenes.[46−49] Although such structures await experimental studies to confirm or deny their viability as true nano-objects, recent discoveries have shown first steps toward the synthesis of compounds with planar boron kernels acting as ligands. A B_6 structural motif is found in the crystal structure of a solid-state phase $Ti_7Rh_4Ir_2B_8$, where the B_6 is sandwiched between two Ti atoms in a bipyramidal fashion.[50] A similar structural motif is

Received: December 22, 2013
Published: March 24, 2014

   dx.doi.org/10.1021/ar400310g | Acc. Chem. Res. 2014, 47, 1349−1358

found in the cluster $[TaB_6Ta]^-$, which has been produced in a molecular beam and characterized via photoelectron spectroscopy (PES) corroborated by theoretical calculations.[51] The study showed an intrinsic connection between the gas phase cluster and the geometric motif for solid materials. Thus, planar boron-based fragments are viable ligands that will likely play an important role in the future of condensed phase coordination chemistry.

Despite significant efforts by computational chemists to probe large boron nanoparticles and two-dimensional sheets, the clusters of boron continue to be the only experimentally assessable species. Clusters exhibit unique size-dependent properties, distinct from molecules and bulk solids. Since little can be determined about the structure and properties of the clusters a priori, accurate characterization relies on synergetic efforts between experimentalists and theoreticians.[52,53] We have demonstrated that joint photoelectron spectroscopic and *ab initio* studies can facilitate determination of the most stable structure of anionic boron clusters (B_n^-, n = 3−24). Accurate thermochemical data on boron clusters from 5 to 13 atoms have been reported by Dixon and co-workers at the CCSD(T) level of theory with large basis sets.[10f,g] The stability of the planar and quasi-planar structures is rationalized via chemical bonding analyses and through invoking concepts of aromaticity and antiaromaticity.[10−22] Our approach is summarized by four steps: (1) *Photoelectron Spectroscopy*. PES is a powerful technique to probe the electronic structure of molecules, providing direct information about electronic states. The experiment is carried out by generating the clusters using laser vaporization and analyzing them in a time-of-flight mass spectrometer. The cluster of interest is mass-selected and photodetached by a laser beam. The photoelectrons are analyzed in a magnetic-bottle photoelectron analyzer.[54,55] (2) *Theoretical global minimum search*. The potential energy surface of the cluster is explored to locate the most viable chemical structures and low-lying isomers. This task is performed using various programs such as the gradient embedded genetic algorithm (GEGA),[56] coalescence kick (CK) method,[13] basin hopping method,[14a,57] and recently developed Cartesian walking (CW) method.[16] (3) *Comparison of the experimental and theoretical vertical detachment energies (VDEs)*. Assignment of the global minimum structure is based on comparison of the measured VDEs from the photoelectron spectra with theoretically calculated VDEs corresponding to the lowest energy isomer(s). (4) *Chemical bonding analysis*. We rationalize the structure of the global minimum through chemical bonding analyses, including the use of the adaptive natural density partitioning (AdNDP) algorithm.[58] These analyses explain what governs the geometric and electronic structure and stability of the cluster at hand. Implementation of the described four-step approach has been reviewed elsewhere[53] on the example of boron clusters up to 15 atoms. The current report focuses on the determination of pure anionic clusters from B_{16}^- to B_{24}^-.[12−18]

Structures of the major contributors to the photoelectron spectra of all the anionic boron clusters studied to date are given in Figure 1 along with their experimentally measured adiabatic detachment energies (ADEs) presented in Figure 2. As is evident, anionic boron clusters remain planar or quasi-planar up to at least 24 atoms. The structures of the low-lying isomers as well as their measured ADE values are reported in the original papers of the B_n^- clusters (n = 3−24).[10−22,53] The following section of this work elucidates our approach to determine the most viable cluster species in more detail, as exemplified by our recent joint study of the B_{24}^- cluster.[18]

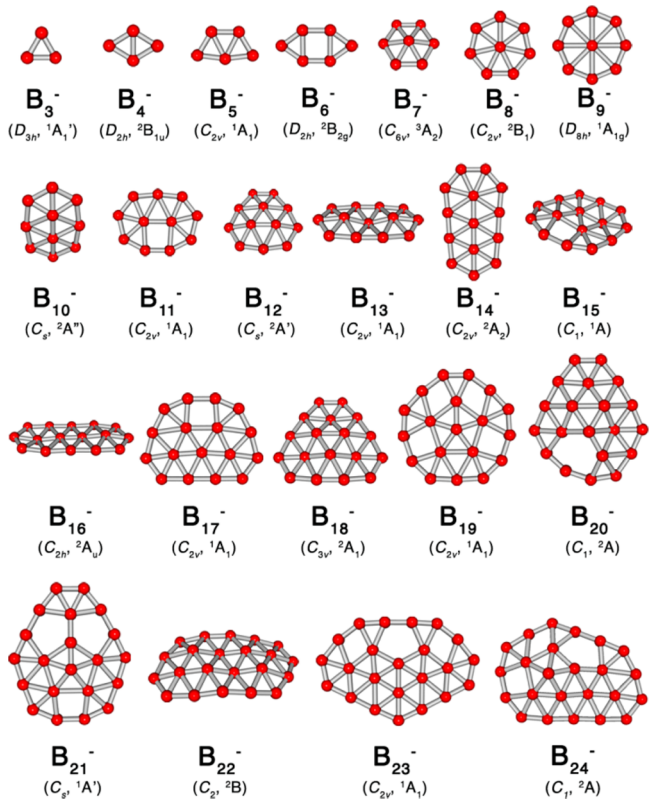

Figure 1. The structures of the major contributors to the photoelectron spectra of B_n^- (n = 3−24).

2. DETERMINING STRUCTURES OF CLUSTERS: EXPERIMENT AND THEORY

We utilized two independent searching methods to find the global minimum structure of B_{24}^-, namely, the CK and CW methods mentioned above. The two searches provided us with a set of low-lying isomers (Figure 3), which were optimized using two density functional theory (DFT) methods: PBE0 and TPSSh. Single-point coupled cluster calculations (ROCCSD and ROCCSD(T)) were carried out subsequently to obtain more accurate relative energies. A beautiful tubular double-ring structure II was found to be the most stable by DFT. This isomer was also suggested to be the most stable structure of B_{24}^- cluster by Nguyen and co-workers in their theoretical work.[59] However, ROCCSD and ROCCSD(T) calculations revealed a quasi-planar structure as the global minimum, isomer I (Figure 3). To unequivocally establish the global minimum structure observed in the experimental cluster beam, we calculate the VDEs of the theoretically predicted global minimum and lowest energy isomers for comparison with the experimental VDEs; these VDEs act as an electronic fingerprint of the cluster structure. The photoelectron spectrum of B_{24}^- is displayed in Figure 4a at 193 nm. The maximum of each photoelectron spectroscopic band corresponds to its experimental VDE. In some cases, the experimental features are the result of a combination of more than one detachment transition (i.e., a summation of multiple VDEs). The PES bands are labeled with X, A, B, C, etc. Band X accounts for the amount of energy needed to detach an electron from the ground state of the anionic cluster, usually resulting in the ground electronic

dx.doi.org/10.1021/ar400310g | Acc. Chem. Res. 2014, 47, 1349−1358

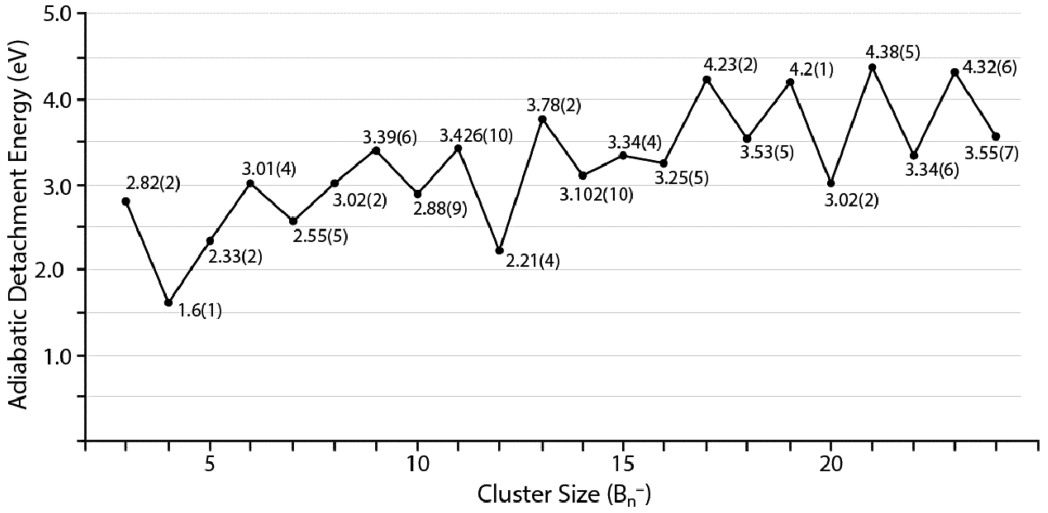

Figure 2. Experimentally measured adiabatic detachment energies (ADEs) of B_n^- (n = 3−24). Energy is given in electronvolts with the reported uncertainty given in parentheses.

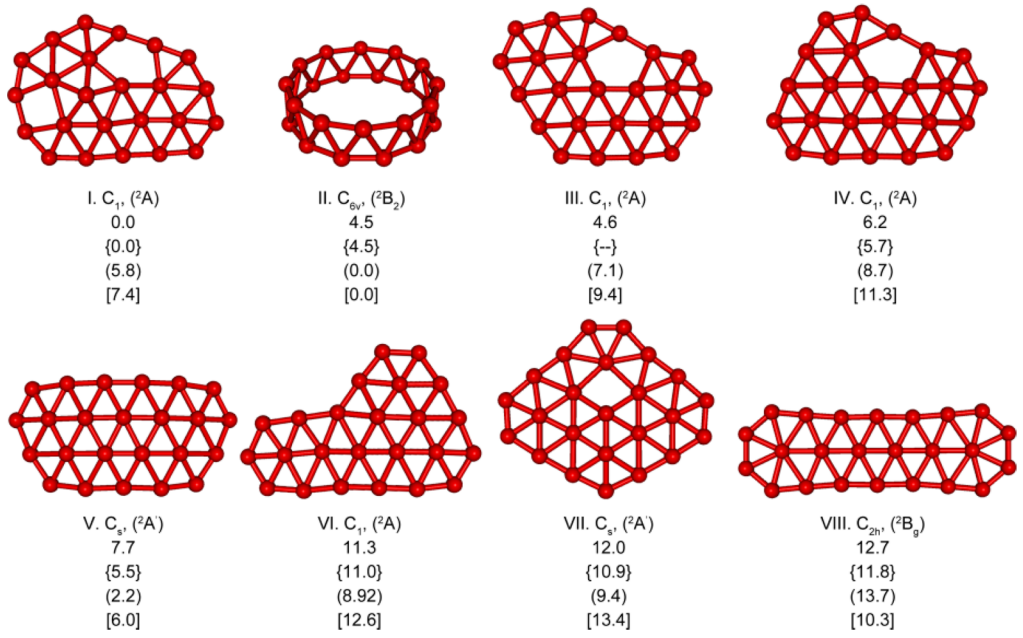

Figure 3. The global minimum and low-lying isomers of B_{24}^-. Relative energies are shown from single-point calculations at ROCCSD/6-311+G(d)//PBE0/6-311+G(d) and ROCCSD(T)/6-311+G(d)//PBE0/6-311+G(d) (in curly brackets), as well those from PBE0/6-311+G(2df)//PBE0/6-311+G(d) (in parentheses) and TPSSh/6-311+G(2df)//TPSSh/6-311+G(d) (in square brackets). The relative energy of isomer III at ROCCSD(T)/6-311+G(d)//PBE0/6-311+G(d) could not be obtained. All relative energies are in kcal/mol.

state of the corresponding neutral species. In most cases, this corresponds to an approximate picture of directly detaching the HOMO electron of the anionic cluster. Bands A, B, C, etc. represent transitions to excited electronic states of the neutral cluster; from the one-electron detachment perspective, these excited states are generated through removal of electrons from the HOMO−1, HOMO−2, etc. molecular orbitals of the anionic cluster. For qualitative comparison, the simulated spectra of isomers I (Figure 4b) and II (Figure 4c) are constructed by fitting the distribution of the VDEs at the PBE0 level of theory with unit-area Gaussian functions of a 0.05 eV full width at half-maximum; excited states were calculated using the TD-DFT approach. No physical principles are strictly used to determine the height and widths in the Gaussian simulation of the PES; agreement with the experimental data is ultimately decided based on the quantitative values of the vertical transitions as presented for B_{24}^- in Table 1. Excellent overall agreement between experiment and theory supports the identification of isomer I as the global minimum for B_{24}^-, whereas the simulated spectrum for the isomer II, the double-ring structure, shows total disagreement with the experimental features. In most cases, such as the B_{24}^- case we have presented herein, the theoretical global minimum corresponds to the observed spectrum, though ultimate determination is decided based on the agreement of the experimental spectra with calculated spectra of the lowest lying isomers. Next we must investigate the question of what makes the global minimum structure stable. Insights into the electronic structure of the global minima of pure boron clusters reveal overall trends of boron chemistry. The reasons for the particular stability of the

dx.doi.org/10.1021/ar400310g | Acc. Chem. Res. 2014, 47, 1349−1358

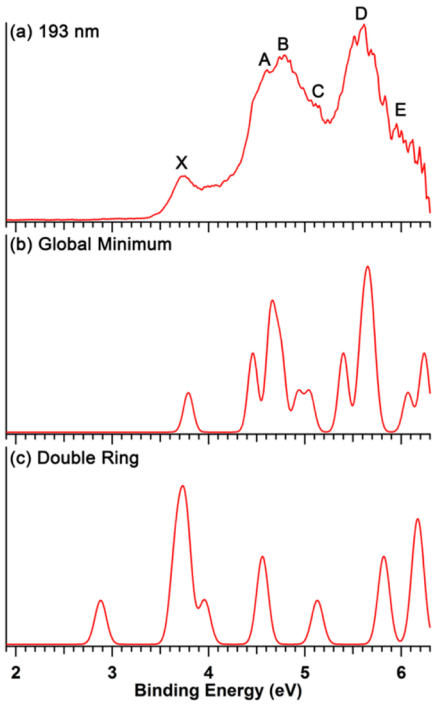

Figure 4. Comparison of the experimental PES spectrum (a) with the simulated PES spectra for the global minimum isomer I (b) and double-ring structure II (c) of B_{24}^- at the PBE0 level of theory.

global minimum structure I of B_{24}^- are described in the original paper.[18] In this Account, we address this question in the following section with discussion on the unique and peculiar global minimum of B_{23}^-, which we have proposed as an all-boron analogue of phenanthrene.[17]

3. ALL-BORON HYDROCARBON ANALOGUES

As mentioned above, the planarity of boron clusters is due to two-dimensional electron delocalization, which raises the concepts of aromaticity, multiple aromaticity/antiaromaticity, and analogies between boron clusters and hydrocarbons. Comparison of the π canonical molecular orbitals (CMOs) of B_{23}^- and phenanthrene (Figure 5a) leads to the conclusion that the B_{23}^- cluster is an all-boron analogue of phenanthrene,[17] a prototypical aromatic hydrocarbon composed of three fused benzene rings. Similarly, the comparison of π CMOs of boron clusters with their hydrocarbon congeners has led to identification of all-boron benzenes B_8^{2-} and B_9^-,[10a] B_{10}, B_{11}^-, and B_{12},[11] and B_{13}^+,[9,23] which were reviewed elsewhere,[53] and all-boron naphthalenes B_{16}^{2-} (shown in Figure 6) and B_{17}^-.[12,13] B_{19}^- was shown to have a chemical bonding picture similar to coronene and [10]annulene[14] (Figure 7); meanwhile bonding in the B_{22}^- cluster is similar to that in anthracene[17] (Figure 8). These bonding concepts provide an intuitive rationale for the unusual stability of boron clusters as two-dimensional structures as well as the stability of the theoretically proposed one-atom thick all-boron two-dimensional material known as the α-sheet,[41] an analogous material to graphene.[60]

4. EXPLAINING CHEMICAL BONDING IN BORON CLUSTERS

To discuss structure from the chemical perspective, one must assess why atoms assume a particular configuration in terms of the bonding. We perform bonding analysis based on CMOs and localized orbitals resulting from the AdNDP algorithm.[58] CMOs are eigenvectors of the model Hamiltonian and are completely delocalized over the cluster. It is possible to discern a localized bonding picture of a molecule through CMO analysis only in the case of very small systems. The CMOs of larger molecules can be useful if one wants to establish an analogy between different species based on the similarity of their CMOs. However, it is not sufficient to understand the bonding in boron clusters, which possess both localized and delocalized bonding. Lipscomb's concept of the three-center–two-electron (3c–2e) bond,[61] along with aromaticity, captures the idea of electron deficiency dictating aspects of boron's bonding. Lipscomb's work on the chemical bonding of the boranes[62] opened the gateway to understanding the chemistry of boron. The AdNDP method is an ideal tool for deciphering the nature of bond localization and delocalization in such clusters; in short it takes advantage of the electron pair as the unit of chemical bonding by partitioning the electron density matrix into *n*c–2e (*n* ranges from 1 to the maximum number of

Table 1. Comparison of the Experimental VDEs and Spectral Features with the Calculated Values for Isomer I (C_1, ^{2}A) of B_{24}^-[a]

			VDE (theory)	
feature	VDE (expt)	final state and electronic configuration	TD-TPSSh	TD-PBE0
X	3.75(7)	^{1}A...$(29a)^2(30a)^2(31a)^2(32a)^2(33a)^2(34a)^2(35a)^2(36a)^2(37a)^0$	3.70	3.79
A	4.61(8)	^{3}A...$(29a)^2(30a)^2(31a)^2(32a)^2(33a)^2(34a)^2(35a)^2(36a)^1(37a)^1$	4.29	4.46
B	4.79(8)	^{1}A...$(29a)^2(30a)^2(31a)^2(32a)^2(33a)^2(34a)^2(35a)^2(36a)^1(37a)^1$	4.48	4.65
		^{3}A...$(29a)^2(30a)^2(31a)^2(32a)^2(33a)^2(34a)^2(35a)^1(36a)^2(37a)^1$	4.51	4.65
		^{3}A...$(29a)^2(30a)^2(31a)^2(32a)^2(33a)^2(34a)^1(35a)^2(36a)^2(37a)^1$	4.64	4.75
C	5.12(8)	^{1}A...$(29a)^2(30a)^2(31a)^2(32a)^2(33a)^2(34a)^2(35a)^1(36a)^2(37a)^1$	4.73	4.93
		^{1}A...$(29a)^2(30a)^2(31a)^2(32a)^2(33a)^2(34a)^1(35a)^2(36a)^2(37a)^1$	4.89	5.05
D	5.62(6)	^{3}A...$(29a)^2(30a)^2(31a)^2(32a)^2(33a)^1(34a)^2(35a)^2(36a)^2(37a)^1$	5.19	5.40
		^{3}A...$(29a)^2(30a)^2(31a)^2(32a)^1(33a)^2(34a)^2(35a)^2(36a)^2(37a)^1$	5.34	5.59
		^{1}A...$(29a)^2(30a)^2(31a)^2(32a)^1(33a)^2(34a)^2(35a)^2(36a)^2(37a)^1$	5.44	5.72
		^{1}A...$(29a)^2(30a)^2(31a)^2(32a)^2(33a)^1(34a)^2(35a)^2(36a)^2(37a)^1$	5.36	5.65
		^{3}A...$(29a)^2(30a)^2(31a)^1(32a)^2(33a)^2(34a)^2(35a)^2(36a)^2(37a)^1$	5.42	5.67
E	5.96(5)	^{1}A...$(29a)^2(30a)^2(31a)^1(32a)^2(33a)^2(34a)^2(35a)^2(36a)^2(37a)^1$	5.85	6.07
		^{3}A...$(29a)^2(30a)^1(31a)^2(32a)^2(33a)^2(34a)^2(35a)^2(36a)^2(37a)^1$	6.02	6.24

[a]All energies are in eV.

dx.doi.org/10.1021/ar400310g | Acc. Chem. Res. 2014, 47, 1349–1358

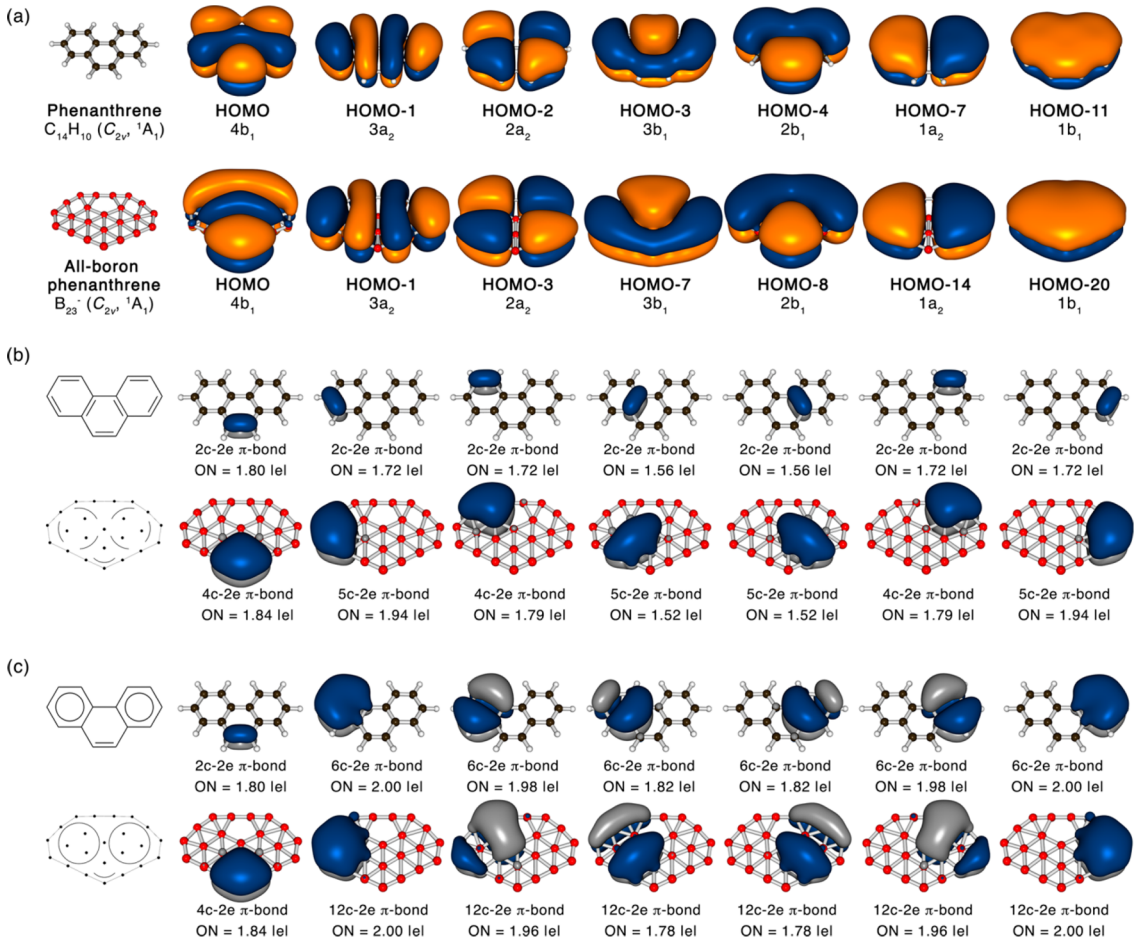

Figure 5. Elucidation of the analogy between phenanthrene and B_{23}^- by comparison of the π electron density: (a) comparison of π canonical molecular orbitals; (b) comparison of the Kekulé π-bonds obtained by the AdNDP method; (c) comparison of the Clar π-bonds obtained by the AdNDP method.

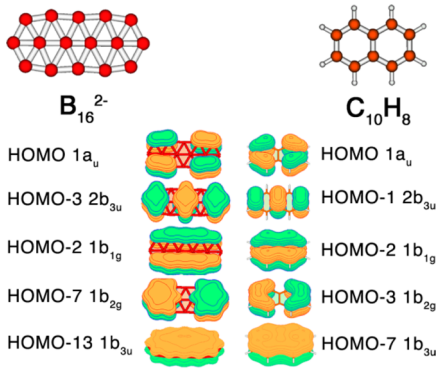

Figure 6. Comparison of the structures and π bonding of B_{16}^{2-} (D_{2h}, ^1A_g) and naphthalene.

atomic centers). We have shown that 2c−2e σ bonds occur at the periphery of all studied planar and quasi-planar boron clusters. For instance, there are 15 2c−2e peripheral B−B σ bonds in B_{23}^- (Figure 9a). The inner atoms are connected to each other and to the peripheral atoms by delocalized bonds (Figure 9b). We have encountered only one exception to the delocalized internal bonding phenomenon: the B_{21}^- cluster was shown to have one inner 2c−2e B−B σ bond.[16] Referring back to the AdNDP analysis of B_{23}^- and its analogy to phenanthrene we note there are $(3 \times 23 + 1) = 70$ valence electrons forming 35 bonds. AdNDP revealed 15 localized B−B σ bonds at the periphery (Figure 9a), 13 delocalized σ bonds inside the cluster (Figure 9b), and 7 delocalized π bonds. Partitioning of the delocalized π electron density in B_{23}^- can be done in two ways: according to Kekulé (Figure 5b) or Clar (Figure 5c) representations of chemical bonding of phenathrene.[17] In Kekulé structure, 2c−2e π-bonds have appreciably lower occupation numbers (ONs), while the Clar representation with delocalized bonds provides a more accurate bonding representation. The analogy between the Kekulé and Clar π bonds of phenanthrene and B_{23}^- shows that the heart-shaped structure is an analogue of the aromatic hydrocarbon.

Aromaticity in chemistry manifests itself as an enhanced stability, high symmetry, and high electron detachment energies in photoelectron spectra; all are attributes of the B_{23}^- cluster. Aromaticity follows the $4n + 2$ Hückel's electron rule. Twenty-six delocalized σ electrons of B_{23}^- satisfy the $4n + 2$ rule for σ aromaticity ($n = 6$), while 14 delocalized π electrons of B_{23}^- satisfy the $4n + 2$ rule for π aromaticity ($n = 3$). Therefore, B_{23}^- is doubly aromatic (σ and π), which explains its stability. B_{23}^- is an example of the significant role of electron delocalization in the formation of planar species that is quite typical in both inorganic and organic chemistry. Such analogies between boron chemistry and hydrocarbons suggest that these two fields of chemistry might mimic each other in unexpected ways.

dx.doi.org/10.1021/ar400310g | Acc. Chem. Res. 2014, 47, 1349−1358

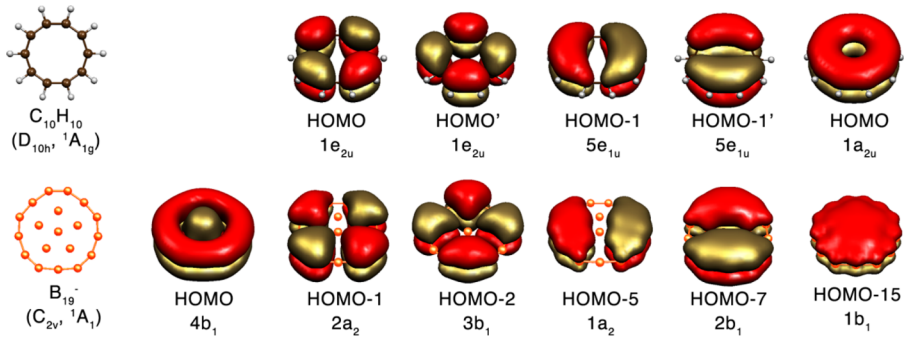

Figure 7. Comparison of the structures and canonical molecular orbitals between [10]annulene ($C_{10}H_{10}$) and the global minimum of B_{19}^-.

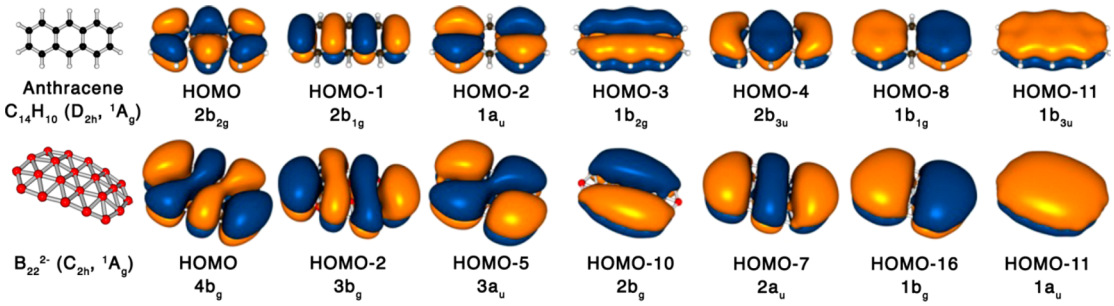

Figure 8. Comparison of the π molecular orbitals in the flattened B_{22}^{2-} cluster with those in anthracene.

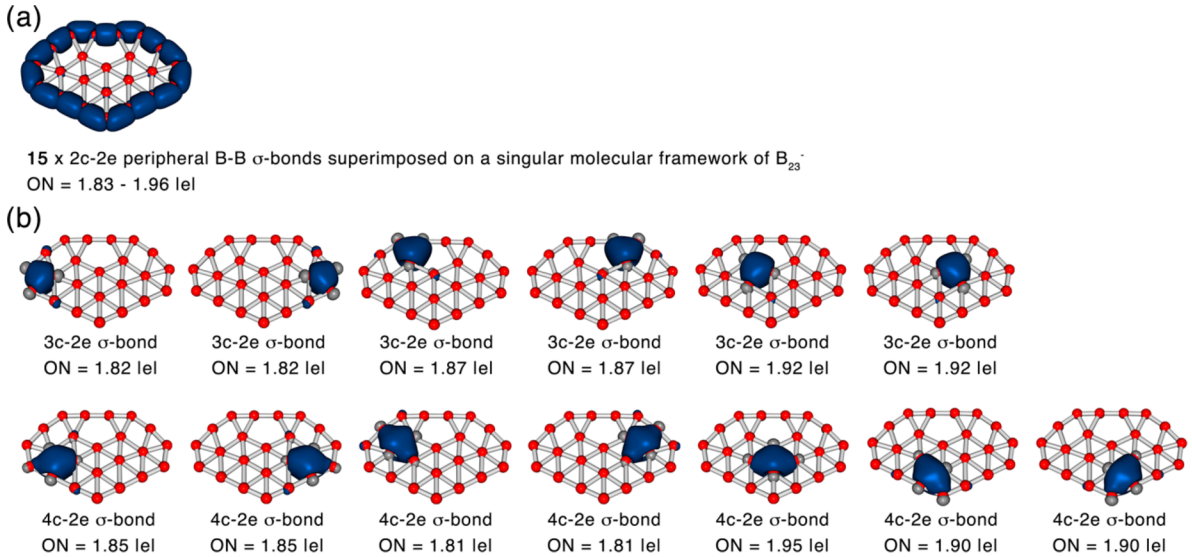

Figure 9. Chemical bonding analysis of the σ electron density of B_{23}^- by the AdNDP method: (a) localized σ bonding is represented by 15 2c−2e peripheral B−B σ bonds; (b) delocalized σ bonding is represented by 13 delocalized σ bonds satisfying the $4n + 2$ rule ($n = 6$) for σ aromaticity. ON stands for occupation number and is equal to 2.00 lel in the ideal case.

5. METAL-CENTERED MONOCYCLIC BORON RINGS

Highly symmetric doubly aromatic boron wheels, B_8^{2-} and B_9^-,[10a,23] have inspired the discovery of a series of metal-centered monocyclic boron rings: $M©B_n^-$.[63] We have developed an electronic design principle capable of predicting which metals can replace the central boron atom in either B_8^{2-} or B_9^- to render a similar doubly aromatic $M©B_n^-$ species (n = 7, 8). Based on the design principle, general geometric and electronic factors in the rational design of the novel borometallic molecular wheels were investigated.[63] We observed and characterized the following octa- and nona-coordinated clusters: $Co©B_8^-$ and $Ru©B_9^-$,[63a] $Ru©B_9^-$ and $Ir©B_9^-$,[63b] and $Fe©B_8^-$ and $Fe©B_9^-$.[63d] Tantalum and niobium were shown to possess a record-breaking coordination number in the planar metal-centered deca-coordinated $Ta©B_{10}^-$ and $Nb©B_{10}^-$ anions.[63c] According to the RCCSD(T) results obtained for these clusters, the wheel-type structures (Figure 10) are the global minima for both anions. These unprecedented results have proven that boron clusters are promising molecules for coordination chemistry as potential new ligands, as well as for material science as new building blocks.

dx.doi.org/10.1021/ar400310g | Acc. Chem. Res. 2014, 47, 1349−1358

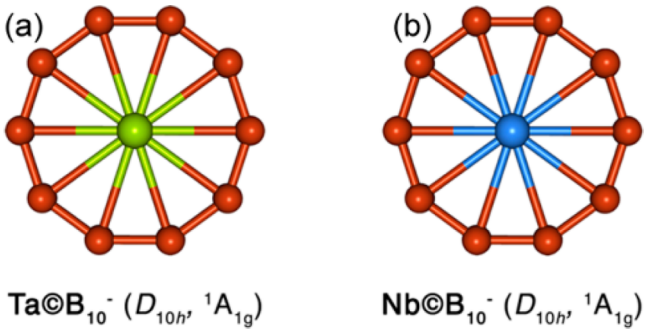

Figure 10. Structures of the two global minimum structures of (a) TaB_{10}^- and (b) NbB_{10}^-, their point group symmetries, and their spectroscopic states.

6. FLUXIONALITY OF BORON CLUSTERS

Some boron clusters were shown to undergo unprecedented internal rotation, the phenomenon that led to the boron clusters' gaining the name of molecular Wankel motors,[64−66] starting with the discovery of the doubly concentric spider-web-like structure of B_{19}^-.[14a] The stability of B_{19}^- was attributed to doubly concentric π aromaticity in two concentric π systems, analogous to coronene.[14] Merino, Heine, and co-workers were the first to demonstrate that B_{19}^- can undergo in-plane internal rotation of the inner centered pentagonal unit with respect to the peripheral boron ring.[64] B_{13}^+ was suggested to be highly fluxional in 1998[8] though the possibility of the internal rotation in this doubly concentric pure boron cluster was demonstrated and explained using chemical bonding analysis only recently.[65] The in-plane rotation was shown to be attainable even at room temperature due to the following factors: similarity of chemical bonds between equilibrium and transition states of the molecular motors and prevalence of delocalized bonding inside of boron clusters.[65] Molecular Wankel motors rotate in both directions and only the application of the circularly polarized infrared laser was shown to achieve a desirable unidirectional rotation rendering a photodriven molecular Wankel motor running on the electronic ground state potential energy surface with a rotational period of a few picoseconds.[66]

7. ELECTRONIC TRANSMUTATION OF BORON INTO CARBON

Addition of an extra electron to boron makes it valence isoelectronic to carbon. B^- behaves as carbon in BH_4^-, assuming a tetrahedral structure similar to that of methane. Such electronic transmutation of boron can be traced in a number of hydrogenated boron clusters.[67−70] Here we discuss this phenomenon as observed in the B_{20} double ring.[15] The bonding in B_{20} has already been discussed in the literature though not from a perspective of electronic transmutation.[28,71] The similarity of chemical bondings of B_{20} and C_{10} are presented in Figure 11. The C_{10} cluster has a ring structure with 10 σ and 10 π delocalized electrons making it doubly (σ and π) aromatic[72] (Figure 11a,b). Each B−B unit in B_{20} contributes four electrons to the localized 2c−2e σ bonds in each chain and leaves two electrons for the delocalized bondings, reminiscent of the C atom in the C_{10} cluster. The analogy between the localized X−X bonds (X = B, C; Figure 11c), delocalized σ (Figure 11d), and delocalized π (Figure 11e) of C_{10} and B_{20} is striking. The only difference is that both boron rings of B_{20} participate in mutual delocalized bonding represented by the overlap of σ and π bonds reminiscent of those in C_{10}.

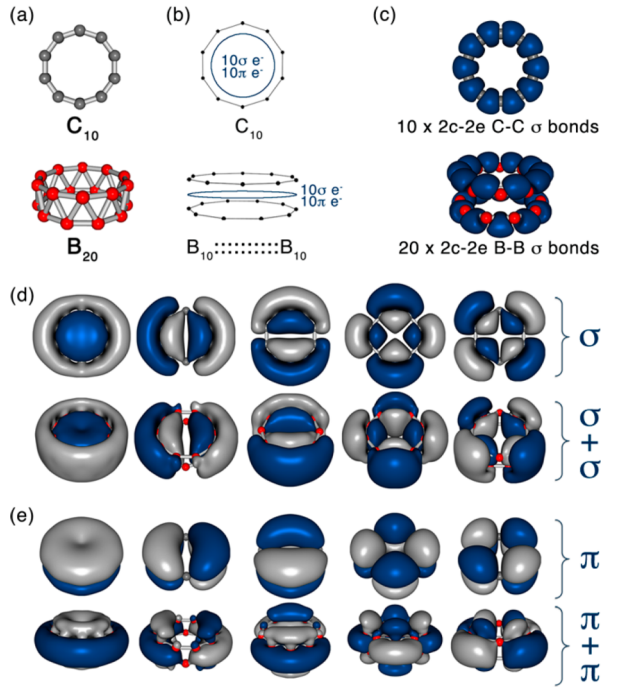

Figure 11. Elucidation of the analogy between the C_{10} ring and the B_{20} double ring. Comparison of (a) structures, (b) schematic representations of bonding, (c) localized Lewis bonds at the periphery, (d) delocalized σ bonds, and (e) delocalized π bonds. The top (bottom) rows correspond to C_{10} (B_{20}).

Therefore, the chemical bonding of B_{20} reveals the tendency of a B−B unit to share a pair of electrons in order to be transmuted to "carbon".

8. CONCLUSIONS AND PERSPECTIVES

In this Account, we have demonstrated the structures of anionic boron clusters can be established through joint photoelectron spectroscopy and *ab initio* studies and discussed some of the exciting insights we have gained about their structures and stability via chemical bonding analyses. We have shown that the anionic pure boron clusters continue to be planar or quasi-planar up to 24 atoms and that this trend is attributed to two-dimensional delocalization rendering aromaticity and multiple aromaticity/antiaromaticity. A number of boron clusters have been shown to be analogous to aromatic hydrocarbons such as benzene, naphthalene, anthracene, phenanthrene, and coronene. Based on the adduced data of wheel-type pure boron clusters, geometric and electronic design principles capable of predicting structures of metal-doped clusters were proposed. Furthermore, unprecedented internal rotation was observed in several boron clusters, a phenomenon that led to the boron clusters' gaining the name of molecular Wankel motors. It has been further shown that this rotation can be achieved in a chosen direction by employing circularly polarized infrared radiation. We are inclined to believe that the peculiar electronic transmutation concept is very effective and helpful in designing new materials with predictable properties.

Though the isolated clusters themselves are exotic species, their chemical bonding, structure, stability, and reactivity could help one rationalize the corresponding properties of novel materials, catalysts, and nanoparticles. We have demonstrated that we can quite reliably explain and even predict the structure of small pure and doped boron clusters. The chemical bonding

dx.doi.org/10.1021/ar400310g | Acc. Chem. Res. 2014, 47, 1349−1358

models developed for boron clusters using ideas of Lewis localization and aromatic delocalization have helped us explain the structure of tentative boron based materials ranging from molecular wheels to two-dimensional boron sheets.

AUTHOR INFORMATION

Corresponding Authors

*E-mail: A.I.Boldyrev@usu.edu.
*E-mail: Lai-Sheng_Wang@brown.edu.

Notes

The authors declare no competing financial interest.

Biographies

Alina P. Sergeeva was born in Sibay, Russia (1986), and received her B. S. (2007) in chemistry from Peoples' Friendship University of Russia in Moscow followed by her Ph.D. (2012) in physical and theoretical chemistry with Prof. Boldyrev at Utah State University in Logan, Utah. She has worked on rationalizing structure, stability, and chemical bonding of pure and doped clusters, isolated and solvated multiply charged anions, organometallic compounds, and solid-state materials. She is currently employed as a postdoctoral research scientist at the Department of Biochemistry and Molecular Biophysics at Columbia University (Center for Computational Biology and Bioinformatics at Howard Hughes Medical Institute).

Ivan A. Popov was born in Sibay, Russia (1987), and obtained his B.S. (2009) and M.S. (2011) diplomas with honors in chemistry with an emphasis in physical chemistry from Peoples' Friendship University of Russia, Moscow. Ivan joined Prof. Boldyrev's group at Utah State University in 2011. He is currently a 3rd year Ph.D. candidate in theoretical physical chemistry focusing on investigation of a novel type of structural transitions in the series of pure and doped clusters, rationalizing chemical bonding in two-dimensional sheets of carbon and boron and solid-state materials.

Zachary A. Piazza was born in Daytona Beach, FL, and obtained his B.S. degree in chemistry from Pace University of New York, NY, in 2009. He is currently a Ph.D. candidate in Prof. Wang's group focusing on the application of theoretical methodologies to solve the structures of boron clusters and the development and implementation of global searching methods for clusters.

Wei-Li Li was born in Hangzhou, China, and obtained her B.S. degree in chemistry from the University of Science and Technology of China in 2009. She is currently a Ph.D. candidate in Prof. Wang's group focusing on experimental and theoretical studies of size-selected nanoclusters.

Constantin Romanescu received his B.S. degree in chemical engineering from Gh Asachi Technical University in Romania and his Ph.D. degree in physical chemistry from Queen's University at Kingston, Ontario, Canada. After a postdoctoral stay at SRI International, Menlo Park, California, he did his second postdoctoral training in Prof. Wang's group at Brown University.

Lai-Sheng Wang received his B.S. degree from Wuhan University in China and his Ph.D. from the University of California at Berkeley. After a postdoctoral stay at Rice University, he took a joint position between Washington State University and Pacific Northwest National Laboratory, then accepted an appointment as Professor of Chemistry at Brown University in 2009. His research group focuses on the investigation of the size-dependent properties of nanoclusters using photoelectron spectroscopy and computational tools, as well as spectroscopic studies of free multiply charged anions and complex solution-phase molecules using electrospray ionization and photodetachment spectroscopy. His group has developed cryogenic ion traps to create cold anions from electrospray for high-resolution spectroscopic studies. His lab has also ventured into bulk syntheses of atom-precise and ligand-protected gold nanoclusters.

Alexander I. Boldyrev was born in Novokuznezk, Russia (1951), and received his B.S./M.S. (1974) in chemistry from Novosibirsk University, his Ph.D. in physical chemistry from Moscow State University, and his Dr. Sci. in chemical physics from Moscow Physico-Chemical Institute (1984). He is currently a professor at the Department of Chemistry and Biochemistry at Utah State University. His current scientific interest is the development of chemical bonding models capable of predicting the structure, stability, chemical bonding, and other molecular properties of pure and mixed main group metal, nonmetal, and metalloid clusters, with the most recent accent on transition metal clusters.

ACKNOWLEDGMENTS

This research was supported by the National Science Foundation (Grant CHE-1263745 to L.S.W. and Grant CHE-1057746 to A.I.B.). Computer, storage, and other resources from the Division of Research Computing in the Office of Research and Graduate Studies at Utah State University are gratefully acknowledged. Supercomputing resources from the center for computation and visualization (CCV) at Brown University, the National Science Foundation sponsored Extreme Science and Engineering Discovery Environment (XSEDE), and the Department of Energy's Environmental Molecular Sciences Laboratory (EMSL) are also gratefully acknowledged.

REFERENCES

(1) Albert, B.; Hillebrecht, H. Boron: Elementary Challenge for Experimenters and Theoreticians. *Angew. Chem., Int. Ed.* **2009**, *48*, 8640−8668.
(2) (a) Decker, B. F.; Kasper, J. S. The Crystal Structure of a Simple Rhombohedral Form of Boron. *Acta Crystallogr.* **1959**, *12*, 503−506. (b) Hoard, J. L.; Sullenger, D. B.; Kennard, C. H. L.; Hughes, R. E. The Structure Analysis of β-Rhombohedral Boron. *J. Solid State Chem.* **1970**, *1*, 268−277. (c) Oganov, A. R.; Chen, J.; Gatti, C.; Ma, Y. Z.; Ma, Y. M.; Glass, C. W.; Liu, Z.; Yu, T.; Kurakevych, O. O.; Solozhenko, V. L. Ionic High-Pressure Form of Elemental Boron. *Nature* **2009**, *457*, 863−867.
(3) (a) Hanley, L.; Whitten, J. L.; Anderson, S. L. Collision-Induced Dissociation and Ab Initio Studies of Boron Cluster Ions: Determination of Structures and Stabilities. *J. Phys. Chem.* **1988**, *92*, 5803−5812. (b) Lu, H.; Li, S. D. Three-Chain B_{6n+14} Cages as Possible Precursors for the Syntheses of Boron Fullerenes. *J. Chem. Phys.* **2013**, *139*, No. 224307.
(4) Kawai, R.; Weare, J. H. Instability of the B_{12} Icosahedral Cluster: Rearrangement to a Lower Energy Structure. *J. Chem. Phys.* **1991**, *95*, 1151−1159.
(5) Ricca, A.; Bauschlicher, C. W. The Structure and Stability of B_n^+ Clusters. *Chem. Phys.* **1996**, *208*, 233−242.
(6) Boustani, I. Systematic Ab Initio Investigation of Bare Boron Clusters: Determination of the Geometry and Electronic Structures of B_n (n=2−14). *Phys. Rev. B* **1997**, *55*, 16426−16438.
(7) Niu, J.; Rao, B. K.; Jena, P. Atomic and Electronic Structures of Neutral and Charged Boron and Boron-Rich Clusters. *J. Chem. Phys.* **1997**, *107*, 132−140.
(8) Gu, F. L.; Yang, X.; Tang, A. C.; Jiao, H.; Schleyer, P. v. R. Structure and Stability of B_{13}^+ Clusters. *J. Comput. Chem.* **1998**, *19*, 203−214.
(9) (a) Fowler, J. E.; Ugalde, J. M. The Curiously Stable B_{13}^+ Cluster and its Neutral and Anionic Counterparts: The Advantages of

Planarity. *J. Phys. Chem. A* **2000**, *104*, 397−403. (b) Aihara, J. B_{13}^+ Is Highly Aromatic. *J. Phys. Chem. A* **2001**, *105*, 5486−5489.
(10) (a) Zhai, H. J.; Alexandrova, A. N.; Birch, K. A.; Boldyrev, A. I.; Wang, L. S. Hepta- and Octa-Coordinated Boron in Molecular Wheels of Eight- and Nine-Atom Boron Clusters: Observation and Confirmation. *Angew. Chem., Int. Ed.* **2003**, *42*, 6004−6008. (b) Zhai, H. J.; Wang, L. S.; Alexandrova, A. N.; Boldyrev, A. I.; Zakrzewski, V. G. Photoelectron Spectroscopy and ab Initio Study of B_3^- and B_4^- Anions and Their Neutrals. *J. Phys. Chem. A* **2003**, *107*, 9319−9328. (c) Zhai, H. J.; Wang, L. S.; Alexandrova, A. N.; Boldyrev, A. I. Electronic Structure and Chemical Bonding of B_5^- and B_5 by Photoelectron Spectroscopy and ab Initio Calculations. *J. Chem. Phys.* **2002**, *117*, 7917−1724. (d) Alexandrova, A. N.; Boldyrev, A. I.; Zhai, H. J.; Wang, L. S.; Steiner, E.; Fowler, P. W. Structure and Bonding in B_6^- and B_6: Planarity and Antiaromaticity. *J. Phys. Chem. A* **2003**, *107*, 1359−1369. (e) Alexandrova, A. N.; Boldyrev, A. I.; Zhai, H. J.; Wang, L. S. Electronic Structure, Isomerism, and Chemical Bonding in B_7^- and B_7. *J. Phys. Chem. A* **2004**, *108*, 3509−3517. (f) Nguyen, M. T.; Matus, M. H.; Ngan, V. T.; Grant, D. J.; Dixon, D. A. Thermochemistry and Electronic Structure of Small Boron and Boron Oxide Clusters and Their Anions. *J. Phys. Chem. A* **2009**, *113*, 4895−4909. (g) Tai, T. B.; Grant, D. J.; Nguyen, M. T.; Dixon, D. A. Thermochemistry and Electronic Structure of Small Boron Clusters (B_n, n = 5 - 13) and Their Anions. *J. Phys. Chem. A* **2010**, *114*, 994−1007.
(11) Zhai, H. J.; Kiran, B.; Li, J.; Wang, L. S. Hydrocarbon Analogs of Boron Clusters: Planarity, Aromaticity, and Antiaromaticity. *Nat. Mater.* **2003**, *2*, 827−833.
(12) Sergeeva, A. P.; Zubarev, D. Y.; Zhai, H. J.; Boldyrev, A. I.; Wang, L. S. A Photoelectron Spectroscopic and Theoretical Study of B_{16}^- and B_{16}^{2-}: An All-Boron Naphthalene. *J. Am. Chem. Soc.* **2008**, *130*, 7244−7246.
(13) Sergeeva, A. P.; Averkiev, B. B.; Zhai, H. J.; Boldyrev, A. I.; Wang, L. S. All-Boron Analogues of Aromatic Hydrocarbons: B_{17}^- and B_{18}^-. *J. Chem. Phys.* **2011**, *134*, No. 224304.
(14) (a) Huang, W.; Sergeeva, A. P.; Zhai, H. J.; Averkiev, B. B.; Wang, L. S.; Boldyrev, A. I. A Concentric Planar Doubly π Aromatic B_{19}^- Cluster. *Nat. Chem.* **2010**, *2*, 202−206. (b) Popov, I. A.; Boldyrev, A. I. Chemical Bonding in Coronene, Isocoronene, and Circumcoronene. *Eur. J. Org. Chem.* **2012**, *18*, 3485−3491.
(15) Kiran, B.; Bulusu, S.; Zhai, H. J.; Yoo, S.; Zeng, X. C.; Wang, L. S. Planar-to-Tubular Structural Transition in Boron Clusters: B_{20} as the Embryo of Single-Walled Boron Nanotubes. *Proc. Natl. Acad. Sci. U. S. A.* **2005**, *102*, 961−964.
(16) Piazza, Z. A.; Li, W. L.; Romanescu, C.; Sergeeva, A. P.; Wang, L. S.; Boldyrev, A. I. A Photoelectron Spectroscopy and Ab Initio Study of B_{21}^-: Negatively Charged Boron Clusters Continue to Be Planar at 21. *J. Chem. Phys.* **2012**, *136*, No. 104310.
(17) Sergeeva, A. P.; Piazza, Z. A.; Romanescu, C.; Li, W. L.; Boldyrev, A. I.; Wang, L. S. A Photoelectron Spectroscopic and Theoretical Study of B_{22}^- and B_{23}^-: An All-Boron Phenanthrene. *J. Am. Chem. Soc.* **2012**, *134*, 18065−18073.
(18) Popov, I. A.; Piazza, Z. A.; Li, W. L.; Wang, L. S.; Boldyrev, A. I. A Combined Photoelectron Spectroscopy and Ab Initio Study of the Quasi-Planar B_{24}^- Cluster. *J. Chem. Phys.* **2013**, *139*, No. 144307.
(19) Alexandrova, A. N.; Zhai, H. J.; Wang, L. S.; Boldyrev, A. I. Molecular Wheel B_8^{2-} as a New Inorganic Ligand. Photoelectron Spectroscopy and Ab Initio Characterization of LiB_8^-. *Inorg. Chem.* **2004**, *43*, 3552−3554.
(20) Alexandrova, A. N.; Boldyrev, A. I.; Zhai, H. J.; Wang, L. S. Photoelectron Spectroscopy and Ab Initio Study of the Doubly-Antiaromatic B_6^{2-} Dianion in the LiB_6^- Cluster. *J. Chem. Phys.* **2005**, *122*, No. 054313.
(21) An, W.; Bulusu, S.; Gao, Y.; Zeng, X. C. Relative Stability of Planar Versus Double-Ring Tubular Isomers of Neutral and Anionic Boron Clusters B_{20} and B_{20}^-. *J. Chem. Phys.* **2006**, *124*, No. 154310.
(22) Zubarev, D. Y.; Boldyrev, A. I. Comprehensive Analysis of Chemical Bonding in Boron Clusters. *J. Comput. Chem.* **2007**, *28*, 251−268.
(23) Fowler, P. W.; Gray, B. R. Induced Currents and Electron Counting in Aromatic Boron Wheels: B_8^{2-} and B_9^-. *Inorg. Chem.* **2007**, *46*, 2892−2897.
(24) Oger, E.; Crawford, N. R. M.; Kelting, R.; Weis, P.; Kappes, M. M.; Ahlrichs, R. Boron Cluster Cations: Transition from Planar to Cylindrical Structures. *Angew. Chem., Int. Ed.* **2007**, *46*, 8503−8506.
(25) Truong, B. T.; Nguyen, M. T.; Nguyen, M. T. Structure of Boron Clusters Revisited, B_n With n=14−20. *Chem. Phys. Lett.* **2012**, *530*, 71−76.
(26) Truong, B. T.; Ceulemans, A.; Nguyen, M. T. Disk Aromaticity of the Planar and Fluxional Anionic Boron Clusters $B_{20}^{-/2-}$. *Chem.—Eur. J.* **2012**, *18*, 4510−4512.
(27) Romanescu, C.; Harding, D. J.; Fielicke, A.; Wang, L. S. Probing the Structures of Neutral Boron Clusters Using Infrared/Vacuum Ultraviolet Two Color Ionization: B_{11}, B_{16}, and B_{17}. *J. Chem. Phys.* **2012**, *137*, No. 014317.
(28) Yuan, Y.; Cheng, L. B_{14}^{2+}: A Magic Number Double-Ring Cluster. *J. Chem. Phys.* **2012**, *137*, No. 044308.
(29) Chen, L. B_{14}: An All-Boron Fullerene. *J. Chem. Phys.* **2012**, *136*, No. 104301.
(30) Szwacki, N. G.; Sadrzadeh, A.; Yakobson, B. I. B_{80} Fullerene: An Ab Initio Prediction of Geometry, Stability, and Electronic Structure. *Phys. Rev. Lett.* **2007**, *98*, No. 166804.
(31) Prasad, D. L. V. K.; Jemmis, E. D. Stuffing Improves the Stability of Fullerenelike Boron Clusters. *Phys. Rev. Lett.* **2008**, *100*, No. 165504.
(32) Sadrzadeh, A.; Pupysheva, O. V.; Singh, A. K.; Yakobson, B. I. The Boron Buckyball and Its Precursors: An Electronic Structure Study. *J. Phys. Chem. A* **2008**, *112*, 13679−13683.
(33) Wang, X. Structural and Electronic Stability of a Volleyball-Shaped B_{80} Fullerene. *Phys. Rev. B* **2010**, *82*, No. 153409.
(34) Sadrzadeh, A.; Yakobson, B. I. The Boron Fullerenes. In *Handbook of Nanophysics*; Sattler, K. D., Ed.; CRC Press: Boca Raton, FL, 2010; Vol. 2, Chapter XLVII, pp 1−9.
(35) Tang, H.; Ismail-Beigi, S. Novel Precursors for Boron Nanotubes: The Competition of Two-Center and Three-Center Bonding in Boron Sheets. *Phys. Rev. Lett.* **2007**, *99*, No. 115501.
(36) Yang, X.; Ding, Y.; Ni, J. Ab Initio Prediction of Stable Boron Sheets and Boron Nanotubes: Structure, Stability, and Electronic Properties. *Phys. Rev. B* **2008**, *77*, No. 041402.
(37) Tang, H.; Ismail-Beigi, S. Self-Doping in Boron Sheets From First Principles: A Route to Structural Design of Metal Boride Nanostructures. *Phys. Rev. B* **2009**, *80*, No. 134113.
(38) Özdoğan, C.; Mukhopadhyay, S.; Hayami, W.; Güvenç, Z. B.; Pandey, R.; Boustani, I. The Unusually Stable B_{100} Fullerene, Structural Transitions in Boron Nanostructures, and a Comparative Study of α- and γ-Boron and Sheets. *J. Phys. Chem. C* **2010**, *114*, 4362−4375.
(39) Tang, H.; Ismail-Beigi, S. First-Principles Study of Boron Sheets and Nanotubes. *Phys. Rev. B* **2010**, *82*, No. 115412.
(40) Yakobson, B. I.; Ding, F. Observational Geology of Graphene, at the Nanoscale. *ACS Nano* **2011**, *5*, 1569−1574.
(41) Galeev, T. R.; Chen, Q.; Guo, J. C.; Bai, H.; Miao, C. Q.; Lu, H. G.; Sergeeva, A. P.; Li, S. D.; Boldyrev, A. I. Deciphering the Mystery of Hexagon Holes in an All-Boron Graphene α-sheet. *Phys. Chem. Chem. Phys.* **2011**, *13*, 11575−11578.
(42) Penev, E. S.; Bhowmick, S.; Sadrzadeh, A.; Yakobson, B. I. Polymorphism of Two-Dimensional Boron. *Nano Lett.* **2012**, *12*, 2441−2445.
(43) Liu, Y.; Penev, E. S.; Yakobson, B. I. Probing the Synthesis of Two-Dimensional Boron by First-Principles Computations. *Angew. Chem., Int. Ed.* **2013**, *52*, 3156−3159.
(44) Singh, A. K.; Sadrzadeh, A.; Yakobson, B. I. Probing Properties of Boron α-tubes by Ab Initio Calculations. *Nano Lett.* **2008**, *8*, 1314−1317.
(45) Saxena, S.; Tyson, T. A. Insights on the Atomic and Electronic Structure of Boron Nanoribbons. *Phys. Rev. Lett.* **2010**, *104*, No. 245502.

(46) Li, H.; Shao, N.; Shang, B.; Yuan, L.; Yang, J.; Zeng, X. C. Icosahedral B_{12}-containing Core-Shell Structures of B_{80}. *Chem. Commun.* **2010**, *46*, 3878−3880.
(47) Zhao, J.; Wang, L.; Li, F.; Chen, Z. B_{80} and Other Medium-Sized Boron Clusters: Core-Shell Structures, Not Hollow Cages. *J. Phys. Chem. A* **2010**, *114*, 9969−9972.
(48) Wang, L.; Zhao, J.; Li, F.; Chen, Z. Boron Fullerenes with 32−56 Atoms: Irregular Cage Configurations and Electronic Properties. *Chem. Phys. Lett.* **2010**, *501*, 16−19.
(49) Li, F.; Jin, P.; Jiang, D. E.; Wang, L.; Zhang, S. B.; Zhao, J.; Chen, Z. B_{80} and $B_{101-103}$ Clusters: Remarkable Stability of the Core-Shell Structures Established by Validated Density Functionals. *J. Chem. Phys.* **2012**, *136*, No. 074302.
(50) Fokwa, B. P. T.; Hermus, M. All-Boron Planar B_6 ring in the Solid-State Phase $Ti_7Rh_4Ir_2B_8$. *Angew. Chem., Int. Ed.* **2012**, *51*, 1702−1705.
(51) Li, W. L.; Xie, L.; Jian, T.; Romanescu, C.; Huang, X.; Wang, L. S. Hexagonal Bipyramidal $[Ta_2B_6]^{-/0}$ Clusters: B_6 Rings as Structural Motifs. *Angew. Chem., Int. Ed.* **2014**, *126*, 1312−1316.
(52) Boldyrev, A. I.; Wang, L. S. All-Metal Aromaticity and Antiaromaticity. *Chem. Rev.* **2005**, *105*, 3716−3757.
(53) Alexandrova, A. N.; Boldyrev, A. I.; Zhai, H. J.; Wang, L. S. All-Boron Aromatic Clusters as Potential New Inorganic Ligands and Building Blocks in Chemistry. *Coord. Chem. Rev.* **2006**, *250*, 2811−2866.
(54) Wang, L. S.; Cheng, H. S.; Fan, J. Photoelectron Spectroscopy of Size-Selected Transition Metal Clusters: Fe_n^-, n = 3−24. *J. Chem. Phys.* **1995**, *102*, 9480−9493.
(55) Wang, L. S.; Wu, H. Probing the Electronic Structure of Transition Metal Clusters From Molecular to Bulk-Like Using Photoelectron Spectroscopy. In *Advances in Metal and Semiconductor Clusters. IV. Cluster Materials*; Duncan, M. A., Ed.; JAI Press: Greenwich, CT, 1998; pp 299−343.
(56) Alexandrova, A. N.; Boldyrev, A. I. Search for the $Li_n^{0/+1/-1}$ (n = 5−7) Lowest-Energy Structures Using the *Ab Initio* Gradient Embedded Genetic Algorithm (GEGA). Elucidation of the Chemical Bonding in Lithium Clusters. *J. Chem. Theory Comput.* **2005**, *1*, 566−580.
(57) Wales, D. J.; Doye, J. P. K. Global Optimization by Basin-Hopping and the Lowest Energy Structures of Lennard-Jones Clusters Containing Up to 110 atoms. *J. Phys. Chem. A* **1997**, *101*, 5111−5116.
(58) Zubarev, D. Y.; Boldyrev, A. I. Developing Paradigms of Chemical Bonding: Adaptive Natural Density Partitioning. *Phys. Chem. Chem. Phys.* **2008**, *10*, 5207−5217.
(59) Pham, H. T.; Duong, L. V.; Pham, B. Q.; Nguyen, M. T. The 2D-to-3D Geometry Hopping in Small Boron Clusters: The Charge Effect. *Chem. Phys. Lett.* **2013**, *577*, 32−37.
(60) Popov, I. A.; Bozhenko, K. V.; Boldyrev, A. I. Is Graphene Aromatic? *Nano Res.* **2012**, *5*, 117−123.
(61) Eberhardt, W. H.; Crawford, B.; Lipscomb, W. N. The Valence Structure of the Boron Hydrides. *J. Chem. Phys.* **1954**, *22*, 989−1000.
(62) Lipscomb, W. N. *Boron Hydrides*; W. A. Benjamin: New York, 1963.
(63) (a) Romanescu, C.; Galeev, T. R.; Li, W. L.; Boldyrev, A. I.; Wang, L. S. Aromatic Metal-Centered Monocyclic Boron Rings: $Co©B_8^-$ and $Ru©B_9^-$. *Angew. Chem., Int. Ed.* **2011**, *50*, 9334−9337. (b) Li, W. L.; Romanescu, C.; Galeev, T. R.; Piazza, Z. A.; Boldyrev, A. I.; Wang, L. S. Transition-Metal-Centered Nine-Membered Boron Rings: $M©B_9$ and $M©B_9^-$ (M = Rh, Ir). *J. Am. Chem. Soc.* **2012**, *134*, 165−168. (c) Galeev, T. R.; Romanescu, C.; Li, W. L.; Wang, L. S.; Boldyrev, A. I. Observation of the Highest Coordination Number in Planar Species: Decacoordinated $Ta©B_{10}^-$ and $Nb©B_{10}^-$ Anions. *Angew. Chem., Int. Ed.* **2012**, *51*, 2101−2105. (d) Romanescu, C.; Galeev, T. R.; Sergeeva, A. P.; Li, W. L.; Wang, L. S.; Boldyrev, A. I. Experimental and Computational Evidence of Octa- and Nona-Coordinated Planar Iron-Doped Boron Clusters: $Fe©B_8^-$ and $Fe©B_9^-$. *J. Organomet. Chem.* **2012**, *721*−*722*, 148−154. (e) Romanescu, C.; Galeev, T. R.; Li, W. L.; Boldyrev, A. I.; Wang, L. S. Geometric and Electronic Factors in the Rational Design of Transition-Metal-Centered Boron Molecular Wheels. *J. Chem. Phys.* **2013**, *138*, No. 134315. (f) Romanescu, C.; Galeev, T. R.; Li, W. L.; Boldyrev, A. I.; Wang, L. S. Transition-Metal-Centered Monocyclic Boron Wheel Clusters ($M©B_n$): A New Class of Aromatic Borometallic Compounds. *Acc. Chem. Res.* **2013**, *46*, 350−358.
(64) Jimenez-Halla, J. O. C.; Islas, R.; Heine, T.; Merino, G. B_{19}^-: An Aromatic Wankel Motor. *Angew. Chem., Int. Ed.* **2010**, *49*, 5668−5671.
(65) Martínez-Guajardo, G.; Sergeeva, A. P.; Boldyrev, A. I.; Heine, T.; Ugalde, J. M.; Merino, G. Unravelling Phenomenon of Internal Rotation in B_{13}^+ Through Chemical Bonding Analysis. *Chem. Commun.* **2011**, *47*, 6242−6244.
(66) Zhang, J.; Sergeeva, A. P.; Sparta, M.; Alexandrova, A. N. Photo-Driven Molecular Wankel Engine B_{13}^+. *Angew. Chem., Int. Ed.* **2012**, *51*, 8512−8515.
(67) Alexandrova, A. N.; Boldyrev, A. I. Arachno, Nido, and Closo Aromatic Isomers of the $Li_6B_6H_6$ Molecule. *Inorg. Chem.* **2004**, *43*, 3588−3517.
(68) Olson, J. K.; Boldyrev, A. I. Electronic Transmutation: Boron Acquiring an Extra Electron Becomes 'Carbon'. *Chem. Phys. Lett.* **2012**, *523*, 83−86.
(69) Li, W. L.; Romanescu, C.; Jian, T.; Wang, L. S. Elongation of Planar Boron Clusters by Hydrogenation: Boron Analogues of Polyenes. *J. Am. Chem. Soc.* **2012**, *134*, 13228−13231.
(70) Li, D. Z.; Chen, Q.; Wu, Y. B.; Lu, H. G.; Li, S. D. Double-Chain Planar D_{2h} B_4H_2, C_{2h} B_8H_2, and C_{2h} $B_{12}H_2$: Conjugated Aromatic Borenes. *Phys. Chem. Chem. Phys.* **2012**, *14*, 14769−14774.
(71) Johansson, M. On the Strong Ring Currents in B_{20} and Neighboring Boron Toroids. *J. Phys. Chem. C* **2009**, *113*, 524−530.
(72) Martín-Santamaría, S.; Rzepa, H. S. Double Aromaticity and Anti-aromaticity in Small Carbon Rings. *Chem. Commun.* **2000**, *2000*, 1503−1504.